The Application of Neural Networks to Control Technological Process

ALENA VAGASKÁ, PETER MICHAL
Department of Mathematics, Informatics and Cybernetics
Faculty of Manufacturing Technologies, TUKE
Presov, SLOVAK REPUBLIC
alena.vagaska@tuke.sk, peter.michal@tuke.sk

IVO BUKOVSKÝ
Department of Instrumentation and Control Engineerin
Faculty of Mechanical Engineering, CTU in Prague
Prague, CZECH REPUBLIC
ivo.bukovsky@fs.cvut.cz

MIROSLAV GOMBÁR, JÁN KMEC
Department of Management
Faculty of Management, University of Presov in Presov
Presov, SLOVAK REPUBLIC
gombar.mirek@gmail.com, jan.kmec@unipo.sk

Abstract—The paper deals with the possibilities of control andoptimization of the technological process of aluminum anodicoxidation using neural networks and Design of Experiments inorder to evaluate and monitor the influence of the input factorson the resulting AAO (Anodic aluminum oxide) film thickness. Italso compares the usage of different neural unit to define therelationship between individual inputs factors and their mutualinteractions on the resulting AAO film thickness at the monitoredcurrent density 4.00 A·dm-2, 5.00 A·dm-2 and 6.00 A·dm-2.

Keywords—neural network; artificial intellience; surfacetreatment; anodizing;

1. Introduction

Pure aluminum and its alloys, such as weight-saving materials, play an increasingly important role of technical, technological and economic terms [1] in the aerospace and automotive industries [2], where lightweight and rigid structure are preferred [3].The usage of these materials for moving parts is limited due to their low abrasion and wear resistance. To improve tribological properties of such materials, the surface of these components is treated by anodic oxidation process, which also improves the corrosion resistance [1], [2]. The thickness of the AAO film formed on the aluminum substrates is one of the main indicators of corrosion protection and overall durability of so prefinished profiles. For these reasons the anodic oxidation of aluminum has received great attention of considerable amount of researchers. For example, the formation of AAO layers was studied in [4], growth rate of the oxide was studied in [5] and structure of the formed AAO layer was investigated in [6]. The basic tool that allows us to observe the effect of input variables (factors) on output variable (response) is Design of Experiments [7, 8, 9, 10]. The optimum selection of process conditions is an extremely important issue as the sedetermine surface quality of the manufactured parts [11, 12, 13, 14]. The mathematical modeling of the process involves several parameters that may lead to difficult analytical solution [15, 16, 17, 18, 19]. On the other hand, the use of artificial intelligence (neural networks theory) for evaluating the experiment results is justified mainly due to higher speed and accuracy of behavior prediction of observed process compared to conventional statistical evaluation methods [20, 21, 22, 23, 24].

2. Experimental

2.1. Preparation of samples

Alloy EN AW 1050 - H24 with dimensions 101x70x1 mm was used for the specimens. Each applied specimen was degreased in a 38.00% solution of NaOH at 55.00 to 60.00 ° C for 2 minutes and stained in a 40.00% solution of NaOH at the temperature 45.00 ° -50.00 ° C for 0.50 min. Consequently, the specimen was immersed in a nitric acid bath (4.00% HNO_3) at the temperature 18.00 to 24.00 ° C for 1.00 minute. Between each operation, the sample was rinsed with distilled water.

2.2. Anodization conditions

The electrolyte solution containing sulphuric acid p.a., oxalic acid p.a. and alumina oxide p.a. was used for anodic oxide process. Individual concentrations were based on the Design of Experiments (DoE) methodology corresponding to the central composite design for six factors, which determined operating conditions of anodizing process (the electrolyte temperature, the size of an applied voltage and duration of oxidation). Tab. 1 presents the conversion of factor levels between coded scale and natural one. Such areas of the sample surface where the current density was 4 $A \cdot dm^{-2}$, 5 $A \cdot dm^{-2}$ or 6 $A \cdot dm^{-2}$ were indicated after the anodizing process was finished. Furthermore, 9 points were indicated at a distance of 5mm, 10mm, 15mm, 20mm, 25mm, 30mm, 35mm, 40mm and 45 mm from the bottom edge of each sample. The thickness of the formed anodic oxide films was measured in these points.

TABLE I. CONVERSION OF FACTORS LEVELS BETWEEN CODED SCALE AND NATURAL ONE

Factors denotation		**Factor level**				
Coded Scale	***Natural Scale***	**-2.37**	**-1**	**0**	**+1**	**+2.37**
x_1	H_2SO_4[mol·l^{-1}]	0.34	1.33	2.04	2.75	3.74
x_2	C_2H2O_4[mol·l^{-1}]	$1.65\cdot10^{-2}$	$7.77\cdot10^{-2}$	$1.22\cdot10^{-1}$	$1.66\cdot10^{-1}$	$2.28\cdot10^{-1}$
x_3	Al^{3+}[mol·l^{-1}]	$6.67\cdot10^{-3}$	$1.85\cdot10^{-1}$	$3.15\cdot10^{-1}$	$4.45\cdot10^{-1}$	$6.23\cdot10^{-1}$
x_4	T[°C]	-1.78	12.00	22.00	32.00	45,78
x_5	t [s]	373.00	1200.00	1800.00	2400.00	3226.00
x_6	U[V]	5.24	8.00	10.00	12.00	14.76

3. The Application of Neural Networks in the Evaluation of Anodizing Process

A higher-order neural unit (HONU), especially the 3rd order HONU [26] based on the iterative Levenberg-Marquardt (LM) algorithm [27] was used to determine the influence of input factors on the thickness of the final AAO layer. This algorithm is often used for training technique of the neural unit. It is a process of updating individual weights **w** in a predetermined number of steps to achieve a minimum difference between the actual and calculated values of observed variable [28]. This process is described by (1) – (8). The vector **u** of neural inputs is created by taking the partial derivatives of each output in respect to each weight (1) – (3). The equation describing the investigated model is the characteristic equation of given type of neural unit (1storder HONU, 2ndorder HONU a 3rdorder HONU) for observed factors x_1, x_2, x_3, x_4, x_5, x_6. The Levenberg-Marquardt algorithm consists in solving (4), where the Jacobian **J** is the matrix of dimension $n\times m$ (5), where n is the length of the input vector **u** of the neural unit (n is the number of neural inputs) and m is the total number of parameters intended for the learning procedure. The vector of neural inputs as well as the Jacobian is defined in the first step of the learning procedure and they remain constant in all subsequent steps of learning. In (4) there is the weight update vector **Δw** that we want to find, **e** is the error vector containing the output errors for each input vector used on training the network, 1/ μ is the Leveberg's damping factor which tell us by how much we should change our network weights to achieve a (possibly) better solution. The $\mathbf{J}^T\cdot\mathbf{J}$ matrix can also be known as the approximated Hessian, the **I** is an identity matrix of diagonal length equal to the number of neural weights (matrix of dimension $n\times n$), μ is the learning rate.

The vector **y'** of neural outputs is defined as the dot product of vectors **w** and **u** (6), the size of the individual weight is set in the first step randomly. After calculating the output vector is calculated error vector **e** as the difference between the actual value of the observed variable and the calculated one by the neural units (6). Then the weight update vector **Δw** is determined by (4). The size of the learning rate μ depends on how quickly and how accurately the neural unit is able to learn. At higher values of learning rate the neural unit will learn faster but there is a risk of instability respectively a risk of model oscillation. At lower values of learning rate the calculation is more accurate but the learning process requires a larger number of iterations [16]. After calculating the weight- updates, the adaptation of the weights of input factors occurs. This is the end of first step (respectively the first iteration) of the learning process of neural unit using iterative Levenberg-Marquardt (LM) algorithm optimization. The learning process of neural units continues by calculating the vector of neural outputs **y** using the new (adapted) weights.

$$u_i = \frac{\partial y_{HONU}}{\partial w_i} \tag{1}$$

$$\mathbf{u} = \begin{bmatrix} u_1 \\ u_2 \\ \vdots \\ u_n \end{bmatrix} \tag{2}$$

$$\mathbf{w} = \begin{bmatrix} w_1 \\ w_2 \\ \vdots \\ w_n \end{bmatrix} \tag{3}$$

$$\mathbf{\Delta w} = \left(\mathbf{J}^T\cdot\mathbf{J} + \frac{1}{\mu}\cdot\mathbf{I}\right)^{-1}\cdot\mathbf{J}^T\cdot\mathbf{e} \tag{4}$$

$$\mathbf{J} = \begin{bmatrix} \mathbf{u}^T{}_1 \\ \mathbf{u}^T{}_2 \\ \vdots \\ \mathbf{u}^T{}_m \end{bmatrix} = \begin{bmatrix} u_{1;1} & u_{2;1} & \cdots & u_{n;1} \\ u_{1;2} & u_{2;2} & \cdots & u_{n;2} \\ \vdots & \vdots & \ddots & \vdots \\ u_{1;m} & u_{2;m} & \cdots & u_{n;m} \end{bmatrix} \tag{5}$$

$$\mathbf{y'} = \mathbf{w}\cdot\mathbf{u} \tag{6}$$

$$\mathbf{e} = \mathbf{y} - \mathbf{y}' \tag{7}$$

$$\mathbf{w} = \mathbf{w} + \Delta\mathbf{w} \tag{8}$$

4. Results and Discussion

Setting of simulation was used as follows. Letter *y* means a mean value of the layer thickness measured in points at a distance of 10.00 mm, 20.00 mm, 30.00 mm and 40.00 mm from bottom margin of each testing sample. Current density was set at 4.00, 5.00 and 6.00 A·dm^{-2}. For learning process were used 36 values of randomly measured thickness for one setting of the current density. Ten remaining values of the thickness were used during model validation process. That value ratio was chosen experimentally, according to goal to find the lowest possible number of training values sufficient enough to provide the prediction model with adequate precision. With the greater amount of training data we were not able to clearly validate the model. During evaluation of the experiment results, it was possible to mathematically describe an influence of the input factors on the resulted thickness of the AAO layer via neural unit. The unit used cubic model with small number of data. According to the theory of the neural networks the third order HONU is able to surely describe highly nonlinear model only via large amount of training data. Respectively, with smaller amount of training data is necessary to choose a neural unit with lower order. When we tried to use lower order neural unit (linear model, quadratic model) a big error of prediction model occurred. The error occurred during the training process and became even greater during validation process. In Tab. 2 it is possible to see how much is the model unable to describe the influence of state values, which were not in training data. In the table are statistical stats of correctness of cubic, quadratic and linear model. The table also contains suitability (or correctness) of usage the particular evaluation models for estimating of the AAO layer thickness. The sum of square errors of 3rd Order HONU was 7.50 times lower than the sum of square errors of 2nd Order HONU at the current density of 4.00 A·dm^{-2}. At the current density of 5.00 A·dm^{-2} the sum of square errors was even 8.33 times lower, and 7.40 times lower at the current density of 6.00 A·dm^{-2}. Usage of 3rd Order HONU is 5.93 times more accurate than 1st Order HONU at the current density of 4.00 A·dm^{-2}, 10.41 times more accurate if the current density was 5.00 A·dm^{-2} and 10.67 times more accurate at the current density of 6.00 A·dm^{-2}. While 3rd Order HONU neural unit was used, correlation index of the input factors and the AAO result thickness reached levels 96.67 %, 97.56 % and 98.33 % at the current densities of 4.00 A·dm^{-2}, 5.00 A·dm^{-2} and 6.00 A·dm^{-2}. In comparison with 2rd Order HONU the correlation index is approximately 7.14% higher and about 12.64% in comparison with results of 1rd Order HONU. Fig.1 shows the simulation error (a difference between measured and calculate value of the AAO layer thickness) of individual mathematical model (1st, 2nd a 3rdorder HONU neural units) developed for the current density of 4.00 A·dm^{-2}.

TABLE II. SELECTED INICATORS OF THE ACCURACY OF DEVELOPED MODELS

Model	Current density [A·dm^{-2}]	SSE [-]	MSE [-]	R^2 [%]	R [%]
Cubic 3rd Order HONU	4.00	87.51	1.90	93.45	96.67
	5.00	62.42	1.36	95.17	97.56
	6.00	45.31	0.98	96.69	98.33
Quadratic 2nd Order HONU	4.00	656.75	14.28	78.79	88.76
	5.00	519.70	11.30	81.03	90.02
	6.00	335.50	7.29	85.30	92.36
Linear 1st Order HONU	4.00	518.69	11.28	68.31	82.65
	5.00	649.87	14.13	78.91	88.83
	6.00	496.92	10.80	69.16	83.16

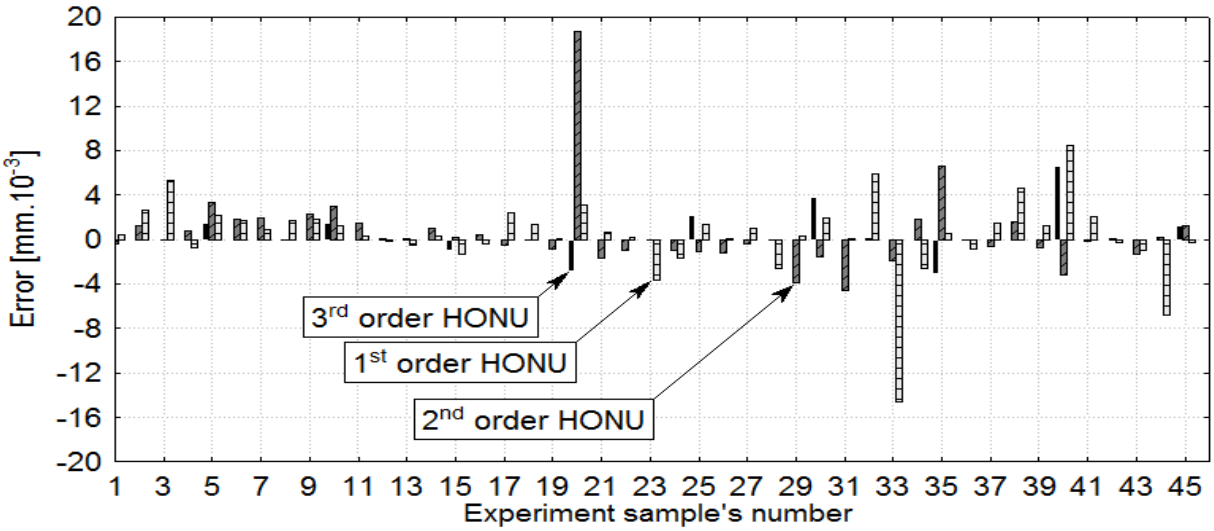

Fig. 1. Simulation error of 1st, 2nd a 3rd order HONU neural units at observed current density of 4.00 A·dm^{-2}

As we can see in the figure, the biggest errors appear in the estimation of AAO layer thickness via 1rd Order HONU, which describes the influence of input parameters using only linear function. The 2rd Order HONU shows lower error of estimation the AAO layer thickness. This neural unit describes the impact on the response by using quadratic function. Usage of that kind of neural unit could be useful in industry to obtain approximate information about input factors influence on the result of technological process. Unfortunately, that neural unit shows the highest absolute calculation error in comparison with other tested neural units. Particularly in estimation of the AAO layer thickness of sample no. 20 the evaluated value is about 18.67 mm·10^{-3} greater than the actual value of measured thickness of the AAO layer. That means a big chance for similarly high error during calculation with the input factors which were not included in the experiment. For that reason, the 2ndOrder HONU neural unit is insufficient for real industry control. The best results are shown by using the 3rdorder HONU neural unit, which describes the influence of input factors on the AAO layer thickness by using quadratic function. In other words, that neural unit is the most nonlinear from tested units and that cause its ability to estimated so complicated model with high precision.

Fig. 2, Fig. 3 and Fig. 4 describe the training process of neural units of 3rdorder HONU and the verification process of the obtained prediction model at current density 4.00 A·dm^{-2} (**Chyba! Nenašiel sa žiaden zdroj odkazov.**), 5.00 A·dm^{-2} (**Chyba! Nenašiel sa žiaden zdroj odkazov.**) and 6.00 A·dm^{-2}(**Chyba! Nenašiel sa žiaden zdroj odkazov.**). From these figures it is clearly seen how all points (values of the AAO layer thickness) used for training are laying on ideally straight line. That means, that the neural unit was able to learn how the input factors influence the resulting AOO layer thickness with almost absolute precision. The sum of square errors reached the value of 1.20·10^{-11} mm^2·10^{-6} during training process at the current density of 4.00 A·dm^{-2}, the value of 1.60·10^{-10} mm^2·10^{-6} at current density of 5.00 A·dm^{-2} and value of 8.38·10^{-9} mm^2·10^{-6} at current density of 6.00 A·dm^{-2}. During the validation process, it results in a difference between the measured value of AAO layer thickness and predicted value of AAO layer thickness, because the neural unit was not trained for that sort of combinations of the input factors.

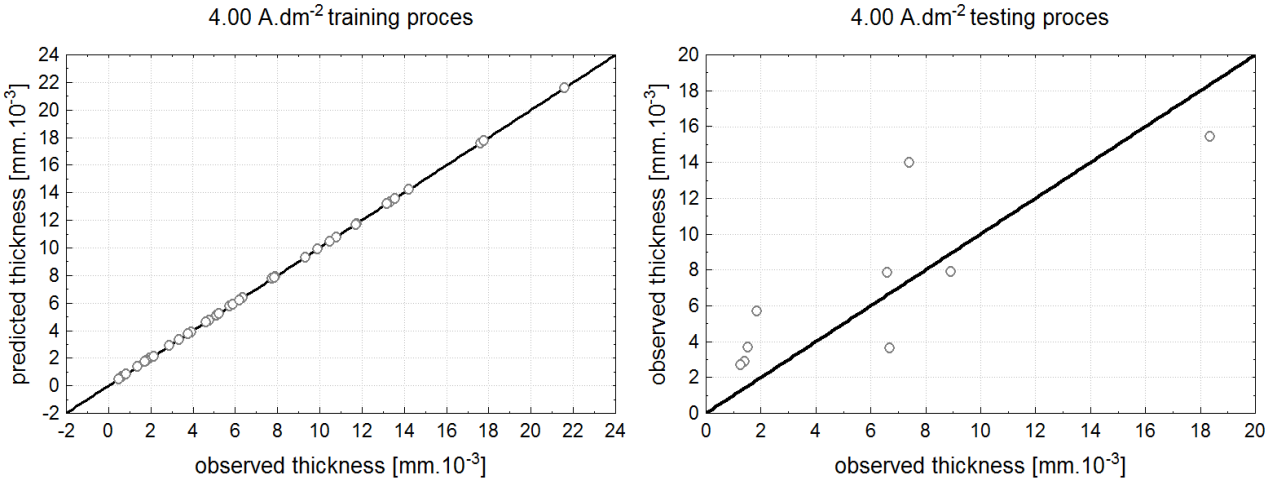

Fig. 2.Training and testing process of 3rd order HONU at current density of 4.00 A·dm^{-2}

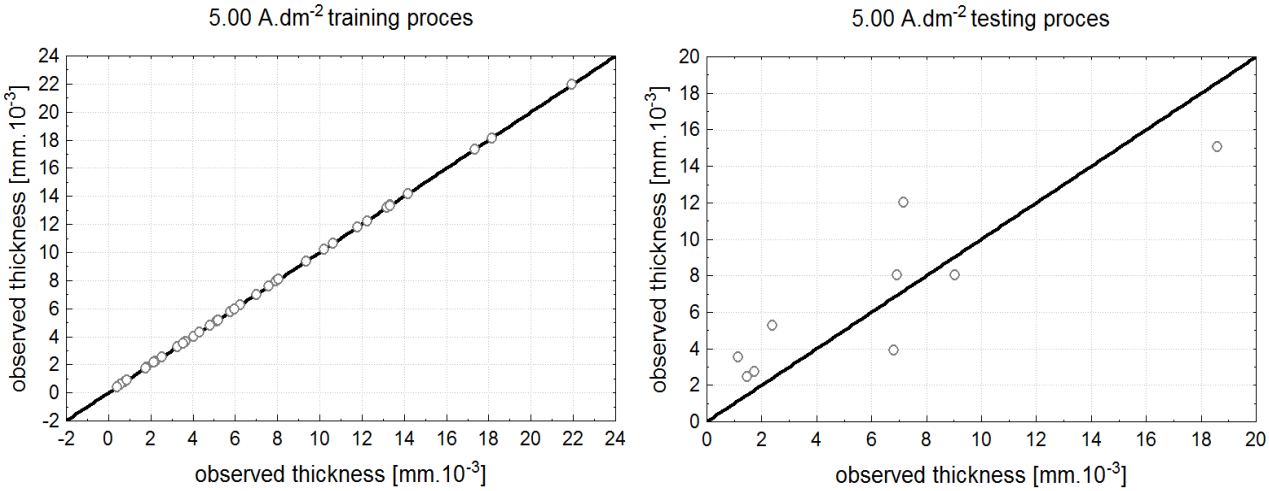

Fig.3.Training and testing process of 3rd order HONU at current density of 5.00 A·dm^{-2}

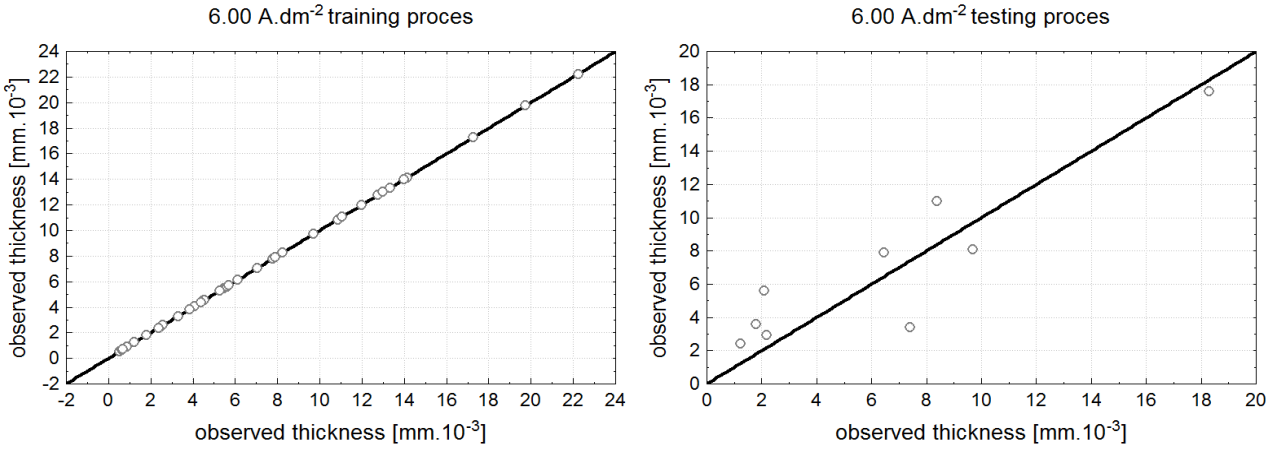

Fig. 4. Training and testing process of 3rd order HONU at current density of 6.00 A·dm^{-2}

Tab. 3 shows the chosen statistical stats of correctness of used models through the validation process for the current densities of 4.00, 5.00 and 6.00 A·dm^{-2}. As is shown, the sum of square errors within model validation process reaches the values of 87.51 mm^2·10^{-6}, 62.42 mm^2·10^{-6} and 45.31 mm^2·10^{-6} according to the individual current densities. Mean absolute error of estimations are 3.12 mm·10^{-3}, 2.63 mm·10^{-}3 and 2.24 mm·10^{-3} for individual current densities 4.00, 5.00 and 6.00 A·dm^{-2}. The confidence interval is 70.23 %, 72.57 % and 82.05 % according to the individual current densities 4.00, 5.00 and 6.00 A·dm^{-2}. These values also mean the accuracy of estimation of formed AAO layer thickness based on various combinations of the input factors.

Using the developed computational models it is also possible to monitor the influence of individual input factors on the final thickness of AAO layer. To illustrate it, the graphical interpretation of dependencies, describing the effect of individual factors on the final thickness of AAO layer at current densities of 4:00, 5:00 and 6:00 A·dm^{-2}, was created. The level of only one factor was varied; the level of the remaining five factors was set at level 0. Fig. 5 – Fig. 10 display the effect of these factors.

The effect of factor x_1 is displayed in Fig. 5, the effect of factor x_2 in Fig. 6, the effect of factor x_3 in Fig. 7, the effect of factor x_4 in Fig. 8, the effect of factor x_5 in Fig. 9 and the effect of factor x_6 in Fig. 10. As seen in Fig. 5 – Fig. 10, the size of the current density has no noticeable effect on the thickness of the AAO layer in those areas where formation of the layer occurs.

TABLE III. SELECTED INDICATORS OF THE ACCURACY OF MODELS IN VALIDATION PROCESS

Model	Current density [A·dm^{-2}]	SSE [-]	MSE [-]	MAE [-]	R^2 [%]	R [%]
Cubic 3rd Order HONU	4.00	87.51	9.72	3.12	70.23	83.81
	5.00	62.42	6.94	2.63	72.57	85.19
	6.00	45.31	5.03	2.24	82.05	90.58

Respectively, the effect of current density is minimal (for boundary conditions, the difference in thickness of the AAO layer is less than 2mm·10^{-3}). When increasing level of factor x_1 (Fig. 5), the electrical conductivity of the electrolyte increases too. On the other hand, when the level of factor x_1 is raised the speed of re-dissolution of alumina formed on the surface of oxidized profile is increased.

Fig. 6 shows that with increasing level of factor x_2, the electrical conductivity of the electrolyte increases (similar to factor x_1). However, the energy required for dissociation of molecules $C_2H_2O_4$ is diminished when factor x_2 is set to its higher level.

From Fig. 7 it can be deduced that low levels of factor x_3 lead to the dissolution of the oxide layer and to the saturation of the electrolyte of aluminum cations Al^{3+}. If the concentration of the aluminum cations in the electrolyte is higher than at the steady state, it results in their migration to the cathode where they are reduced to atomic aluminium and the system energy is decreased.

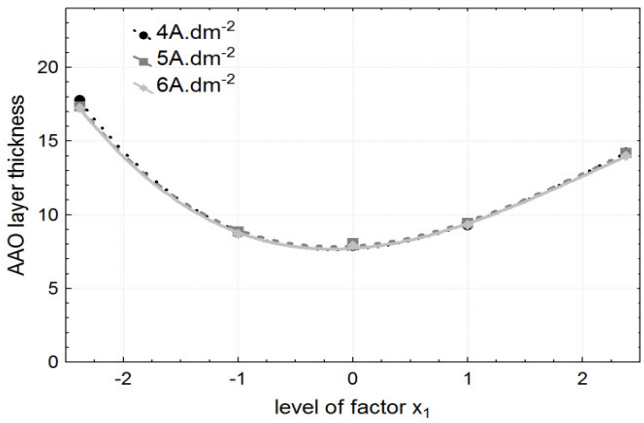

Fig. 5 Effect of factor x_1 on the thickness of AAO layer at given conditions x_2=0 ($1.22 \cdot 10^{-1}$ mol·l^{-1}), x_3=0 ($3.15 \cdot 10^{-1}$ mol·l^{-1}), x_4=0 (22.00 °C), x_5=0 (1800.00 s), x_6=0 (10.00 V)

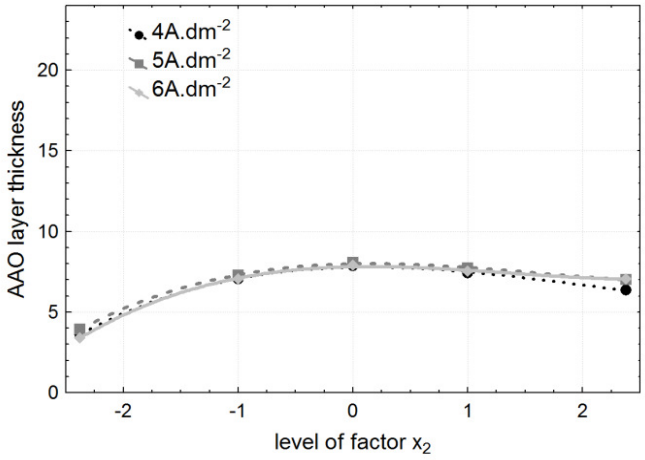

Fig. 6 Effect of factor x_2 on the thickness of AAO layer at given conditions x_1=0 ($2.04 \cdot 10^{-1}$ mol·l^{-1}), x_3=0 ($3.15 \cdot 10^{-1}$ mol·l^{-1}), x_4=0 (22.00 °C), x_5=0 (1800.00 s), x_6=0 (10.00 V)

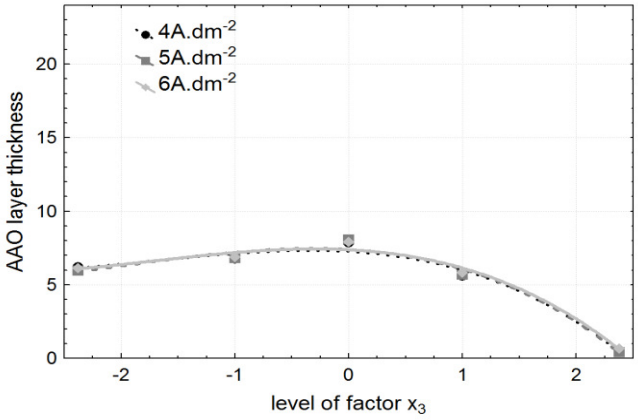

Fig. 7 Effect of factor x_3 on the thickness of AAO layer at given conditions x_1=0 ($2.04 \cdot 10^{-1}$ mol·l^{-1}), x_2=0 ($1.22 \cdot 10^{-1}$ mol·l^{-1}), x_4=0 (22.00 °C), x_5=0 (1800.00 s), x_6=0 (10.00 V)

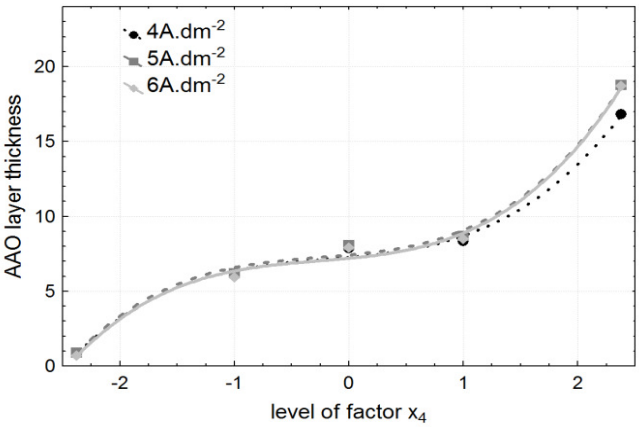

Fig. 8 Effect of factor x_4 on the thickness of AAO layer at given conditions x_1=0 ($2.04 \cdot 10^{-1}$ mol·l^{-1}), x_2=0 ($1.22 \cdot 10^{-1}$ mol·l^{-1}), x_3=0 ($3.15 \cdot 10^{-1}$ mol·l^{-1}), x_5=0 (1800.00 s), x_6=0 (10.00 V)

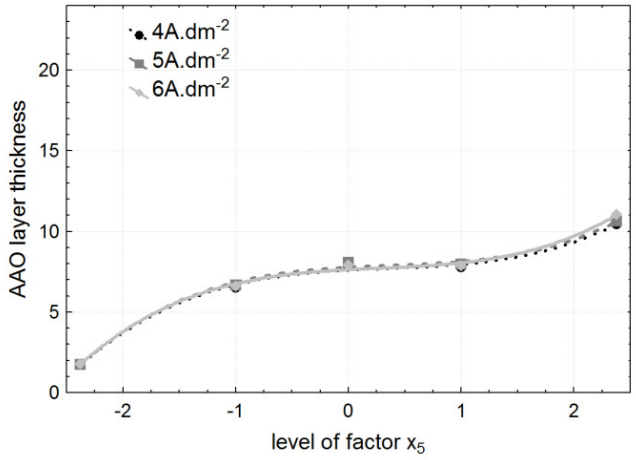

Fig. 9 Effect of factor x_5 on the thickness of AAO layer at given conditions x_1=0 ($2.04 \cdot 10^{-1}$ mol·l^{-1}), x_2=0 ($1.22 \cdot 10^{-1}$ mol·l^{-1}), x_3=0 ($3.15 \cdot 10^{-1}$ mol·l^{-1}), x_4=0 (22.00 °C), x_6=0 (10.00 V)

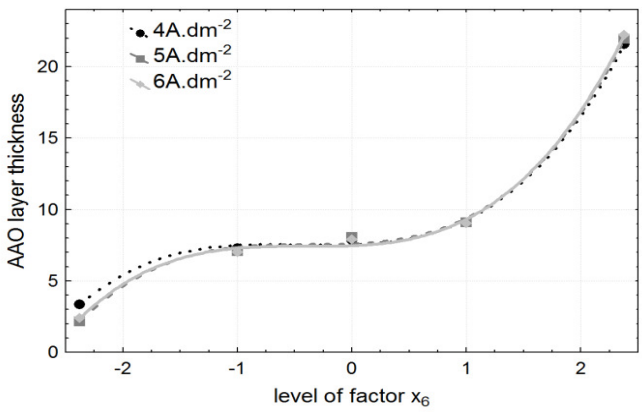

Fig. 10 Effect of factor x_6 on the thickness of AAO layer at given conditions x_1=0 ($2.04 \cdot 10^{-1}$ mol·l^{-1}), x_2=0 ($1.22 \cdot 10^{-1}$ mol·l^{-1}), x_3=0 ($3.15 \cdot 10^{-1}$ mol·l^{-1}), x_4=0 (22.00 °C), x_5=0 (1800.00 s)

The electrolyte conductivity strongly improves with increasing level of factor x_4 (Fig. 8). This is inferred from the fact that the system energy is higher at higher temperatures and therefore chemical reactions proceed more rapidly. On the other hand, the increasing level of factor x_4 enhances the aggressive effects of the electrolyte on the formed AAO layer. Similarly, the layer thickness is increased by increasing level of factor x_5 (Fig. 9) because the layer is formed a longer time. Since factor x_6 determines the strength of such oxygen anions that are attracted to the anode, the thickness of the formed AAO layer also increases with increasing level of factor x_6.

5. Conclusion

As shown by the evaluation of experimental results presented above, the use of neural networks based on the iterative Levenberg-Marquardt (LM) optimization algorithm

provides a wide range of options to control the anodizing process. There are several reasons for this. First and foremost, there is a pressing need to produce the right product at the right time, and here the use of neural networks comes in very handy. We can quickly and simply describe the behavior of the monitored system. By using the neural unit of 3rd order HONU it was possible to describe the influence of input factors on the thickness of final AAO layer at defined current densities 4.00 $A \cdot dm^{-2}$, 5.00 $A \cdot dm^{-2}$ and 6.00 $A \cdot dm^{-2}$ with confidence interval of 93.45%, 95.17% and 96.69%. This neural unit allowed us to monitor the impact of input factors on the final thickness of the AAO layer. It also provide us another way of understanding and expressing the process behavior by graphical representation of how a response (the thickness of AAO layer) may change due to changing values of factors $x_1 - x_5$ and their interactions.

Acknowledgment

The research work is supported by the Project of the Structural Funds of the EU, Operational Programme Research and Development, Measure 2.2 Transfer of knowledge and technology from research and development into practice. Title of the project: „Research and development of intelligent nonconventional actuators based on artificial muscles", ITMS code: 26220220103.

References

[1] J. Baumeister, J. Banhart, M. Weber, "Aluminium foams for transport industry," Materials & Design, vol. 18, no. 4, 1997, pp. 217-220

[2] F. King, "Aluminium and its alloys," UK: Ellis Horwood Limited, 1987

[3] L. A. Dobrza´nski, M. Krupinski, J. H. Sokolowski, "Computer aided classification of flaws occurred during casting of aluminum," Journal of Materials Processing Technology 167, 2005, pp. 456-462

[4] W. Mingliang, L. Yinong, Y. Hong, "A unified thermodynamic theory for the formation of anodized matal oxide," Structures Electrochimica Acta, vol. 62, 2012, pp. 424-432

[5] G. K. Singh, A. A. Golovin, I. S. Aranson, V. M. Vinokur, "Formation of nanoscale pore arrays during anodization of aluminum," Europhysics Letters, vol. 70(6), 2005, pp. 836-842

[6] Z. Meng, S. I. Masatoshi, J. Himendra, "Influence of desiccation procedures on the surface wettability and corrosion resistance of porous aluminium anodic oxide films," Sorrosion Science, vol. 55, 2012, pp. 332-338

[7] M. Gombár, A. Vagaská, J. Kmec, P. Michal, "Microhardness of the coatings created by anodic oxidation of aluminium," Applied Mechanics and Materials," vol. 308, 2013, pp. 95-100 ISSN 1660-9336

[8] A. Vagaská, M. Gombár, J. Kmec, P. Michal, "Statistical analysis of the factors effect on the zinc coating thickness," Applied Mechanics and Materials, vol. 378, 2013, pp. 184-189

[9] P. Michal, M. Gombár, A. Vagaská, J. Piteľ, J. Kmec, "Experimental study and modeling of the zinc coating thickness," Advanced Materials Research, vol. 712-715, 2013, pp. 382-386

[10] A. Panda, J. Jurko, M. Džupon, I. Pandová, "Optimalization of heat treatment bearings rings with goal to eliminate deformation of material," Chemické listy (Chemicla Letters), vol. 105, no. S. (2011)

[11] M. Badida, M. Gombár, L. Sobotová, J. Kmec, "Determination of electroless deposition by chemical nickeling," In: Environmental and Light Industy Technologies, 3rd Int. Joint Conference, 2012, Budapest, Hungary – Budatest: Óbuda University, 2012, p. 27-38,

[12] Ľ. Straka, I. Čorný, J. Boržíková, "Analysis of heat – affected zone depth of sample surface at electrical discharge machining eith brass wire electrode," Strojarstvo: Journal for Theory and Application in Mechanical Engineering, vo. 51, 2009, No. 6, pp. 633-640

[13] M. Gombár, L. Sobotová, M. Badida, J. Kmec, "The comparison of possibilities at using of different electrolytes in the process of anodizing aluminium," Metalurgija, vol. 53, No. 1, 2014, p. 47-50 ISSN 0543-5846

[14] N. Kobasko, "Intense Hardening of Optimal Hardenability Steels Saves Alloy Elements, Energy, Improves Service Life of Machine Components and Makes Environment Cleaner," In: Advances in Modern Mechanical Engineering, FLUIDSHEAT ´13, Croatia 2013, published by WSEAS Press, ISSN: 2227-4596

[15] J. Mižáková, J. Piteľ, "The numerical approximation of function of transient response," In: Matematičeskije metody v technike I technologijach. Tom 7. – Jaroslavľ: Jaroslavskij gosudarstvennyj techničeskij univesitet, 2007, pp. 243-244, ISBN 5230207094

[16] J. Mižáková, "The support of the applied mathematics by chosen programming languages," In. 7. Mathematical workshop, Brno: VUT, 2008, pp. 1-4, ISBN 9788021437272

[17] S. Hrehová, A. Vagaská, "Application of fuzzy principles in evaluating quality of manufacturing process," WSEAS Transaction on Power Systems, vol. 7, No. 2, 2012, pp. 50-59, ISSN 1790-5060

[18] A. Macurová, S. Hrehová, "Some properties of the pneumatic artficial muscle expressed by the nonlinear differential equation," Advanced Materials Research, vol. 658, 2013, Trans Tech Publications Switzerland, p. 376-379, ISSN 1022-6680

[19] S. Hrehová, "Solution of differential equation using a support of some software programs," In. Chapters about Solutions Differential Equations Systems and Some Applications Differential Equations, Brno: Tribun eU, 2009, pp. 59-70, [1.45]

[20] Durmus Karazel, "Prediction and control of surface roughness in CNC lathe using artificial neural network," Journal of Materials Processing Technology, vol. 209, 2009, pp. 3125-3137

[21] L. E. Zárate, F. R. Bittencout, "Representation and control of the cold rolling process through artificial neural networks via sensitivity factors," Journal of Materials Processing Technology 197, 2008, pp. 344-362

[22] A. M. Hassan, A. Alrashdan, M. T. Hayajneh, A. T. Mayyas, "Prediction of density, porosity and hardness in aluminum-copper-based composite materials using artificial neural network," Journal of Materials Processing Technology, vol. 209, 2009, pp. 894-899

[23] J. Piteľ, J. Mižák, "Computational intelligence and low cost sensors in biomass combustion process, Proceedings of the 2013 IEEE (SSCI), Symposium Series on Somputational Intelligence in Control and Automation (CICA), Singapore: IEEE, 2013, pp. 165-168

[24] A. Hošovský, K. Židek, C. Oswald, "Hybridized GA-optimatization of neural dynamic model for nonlinear process, Proceedings of the 2012 13th Intern. Carpathian Control Conference (ICCC), Košice: IEEE, 2012, pp. 227-232

[25] M. Gupta, i. Bukovsky, N. Homma, M. G. A. Solo, Z. G. Hou, "Fundamentals of higher order neural networks for modeling and simulation," Artificial Higher Order Neural Networks for Modelin and Simulation, ed. M. Zhang, IGI Global, 2012

[26] I. Bukovsky, M. Lepold, J. Bila, "Quadratic neural unit and its network in validation of process data of steam turbine loop and energetic boiler," WCCI 2010, IEEE Int. Joint. Conf. on Neural Networks, IJCNN, Barcelona, Spain, 2010

[27] R. Rodriguez, I. Bukovsky, N. Homma, "Potentials of quadratic neural unit for applications," Int. Journal of Software Science and Computational Intelligence (IJSSCI), vol. 3, issue 3, IGI Global, Publishing, Hershey PA, USA, 2011, pp. 1-12, ISSN 1942-9045

[28] I. Bukovsky, N. Homma, L. Smetana, R. Rodriguez, M. Mironovova, S. Vrana, "quadratic neural unit is a good compomise between linear models and neural networks for industrial applications, ICCI 2010, The 9th IEEE Inter. Conference on Cognitive Informaics, Tsinghua University, Beijing, China, July 7-9, 2010